



Quantification of impacts between 1.5 and 4 °C of global warming on flooding risks in six countries

Yi He¹ · Desmond Manful¹ · Rachel Warren¹ · Nicole Forstehäusler¹ · Timothy J. Osborn² · Jeff Price¹ · Rhosanna Jenkins¹ · Craig Wallace² · Dai Yamazaki³

Received: 26 March 2020 / Accepted: 10 December 2021
© The Author(s) 2021

Abstract

We project climate change induced changes in fluvial flood risks for six global warming levels between 1.5 and 4 °C by 2100, focusing on the major river basins of six countries. Daily time series of precipitation, temperature and monthly potential evapotranspiration were generated by combining monthly observations, daily reanalysis data and projected changes in the five CMIP5 GCMs also selected in the ISI-MIP fast track project. These series were then used to drive the HBV hydrological model and the CaMa-Flood hydrodynamic model to simulate river discharge and flood inundation. Our results indicate that return periods of 1 in 100-year floods in the late twentieth century (Q100-20C) are likely to decrease with warming. At 1.5 °C warming, 47%, 66%, 27%, 65%, 62% and 92% of the major basin areas in Brazil, China, Egypt, Ethiopia, Ghana and India respectively experience a decrease in the return period of Q100-20C, increasing to 54%, 81%, 28%, 82%, 86% and 96% with 4 °C warming. The decrease in return periods leads to increased number of people exposed to flood risks, particularly with 4 °C warming, where exposure in the major river basin areas in the six countries increases significantly, ranging from a doubling (China) to more than 50-fold (Egypt). Limiting warming to 1.5 °C would avoid much of these increased risks, resulting in increases ranging from 12 to 1266% for the 6 countries.

Keywords Fluvial flooding · Climate change and warming · HBV · CaMa-Flood · CMIP5

This article is part of the topical collection “Accrual of Climate Change Risk in Six Vulnerable Countries”, edited by Daniela Jacob and Tania Guillén Bolaños

✉ Yi He
yi.he@uea.ac.uk

¹ Tyndall Centre for Climate Change Research, School of Environmental Sciences, University of East Anglia, Norwich Research Park, Norwich NR4 7TJ, UK

² Climatic Research Unit, School of Environmental Sciences, University of East Anglia, Norwich Research Park, Norwich NR4 7TJ, UK

³ Institute of Industrial Science, The University of Tokyo, Tokyo 153-8505, Japan

1 Introduction

Floods cause thousands of fatalities and huge economic losses every year. The global direct economic losses due to floods are over \$1 trillion and more than 220,000 people lost their lives between 1980 and 2013 (Winsemius et al. 2016). Nearly 1 billion people live in floodplains due to convenient access to freshwater resources, fertile lands, protection barriers and navigable corridors (Di Baldassarre et al. 2013; Alfieri et al. 2017). The intensification of the hydrological cycle due to global warming and potentially increased extreme rainfall have led to growing concerns about future flood risks and their impacts on the human societies (Alfieri et al. 2017). It is anticipated that frequencies and magnitudes of floods will become more severe due to global warming in most world regions (Alfieri et al. 2017). Damages due to fluvial flooding have also been increasing due to population growth, increased proximity to flood prone areas and economic activities (Kundzewicz et al. 2014).

Several previous studies have focused on global scale projections of changes in flood frequency under climate change. These generally project increases (with regional variation) in flooding and human exposure to flood risk, regardless of the risk metric, warming scenarios or population projections used. For example, Arnell et al. (2019a, b) found that the global average chance of the 50-year return period river flood increases from 2 to 2.4% at 1.5 °C and 5.4% at 4 °C of global warming. Dottori et al. (2018) found that human losses from flooding could rise by 70–83% with an uneven regional distribution. They projected the strongest rise in the population exposed to flooding in Asia and parts of Africa, South America and western Europe. Arnell et al. (2018) noted that although exposure to flooding is projected to increase when aggregated globally, many CMIP5 GCMs suggest a reduction in flood exposure at 4 °C in some regions (particularly where warming reduces flood peaks from snowmelt in Europe, Russia and the USA). Alfieri et al. (2017) estimated the population exposure to the current 1 in 100-year flood could reach up to 500 million by 2100. Hirabayashi et al. (2013) projected an increase in flood frequency across large areas of South Asia, Southeast Asia, Northeast Eurasia, eastern and low-latitude Africa, and South America, and decreases in many regions of northern and eastern Europe, Anatolia, Central Asia, central North America and southern South America. They concluded the increase in global flood exposure is due mainly to increased exposure in many low-latitude regions, particularly Asia and Africa. In the study by Jongman et al. (2012), the global total population exposed to a 1 in 100-year flood is simulated to reach 1.05 billion in 2050 and this number could well be underestimated as they assumed the hazard area remains constant over time. Milly et al. (2002) found that future changes of 1 in 100-year flood will increase in almost all the 29 major river basins in the world.

The abovementioned studies have highlighted particularly large increases in flood risk in Asia and Africa. Several studies focused on individual river basins or countries (e.g. te Linde et al. 2008; Dankers and Feyen 2008; van Pelt et al. 2009; Veijalainen et al. 2010; Kay and Jones 2012; Cloke et al. 2013; Huang et al. 2013; Ying et al. 2014; Wu et al. 2017) mostly in Europe and China. Direct comparison at the country level is impeded by their use of different models, climate scenarios, baseline and future time periods, and hazard metrics. This study aims to quantify flood risks due to global warming and make the results comparable at the country level by using a consistent set of models, climate scenarios, baseline and future time periods, and hazard metrics. This study selected six countries all considered to be vulnerable to climate change. They are Egypt, Ethiopia, Ghana, China, India and Brazil. They are selected from several continents, spanning different levels of development, and range considerably in size. They are merely examples and the method

could be applied to other countries in the future. Section 2 describes the climate forcing data, the models used in simulating floods, and the metrics used for assessing flood risks. Results are presented in Section 3 followed by the discussion of results in Section 4. Section 5 provides a conclusion.

2 Data and methods

2.1 Climate forcing data

The meteorological inputs required to force the hydrological model (daily precipitation, P ; daily temperature, T ; and monthly potential evapotranspiration, ET) were generated by combining monthly observations, daily reanalysis data, and projected changes in climate from general circulation model (GCM) climate models. The projected changes in climate for the specific warming levels considered here are $< 1.5\text{ }^{\circ}\text{C}$, $< 2.0\text{ }^{\circ}\text{C}$ (which denote aiming to stay below $1.5\text{ }^{\circ}\text{C}$ and $2\text{ }^{\circ}\text{C}$ in 2100, respectively, with 66% probability), exactly $2.5\text{ }^{\circ}\text{C}$, $3.0\text{ }^{\circ}\text{C}$, $3.5\text{ }^{\circ}\text{C}$ and $4.0\text{ }^{\circ}\text{C}$ relative to pre-industrial levels. In this paper, they are referred to as $< 1.5C$, $< 2C$, $2.5C$, $3C$, $3.5C$ and $4C$, respectively. To sample the uncertainty in regional climate change projection, we use patterns of change simulated by five CMIP5 GCMs. The five selected were those used previously by the ISI-MIP fast track project (Warszawski et al. 2014), namely MIROC-ESM-CHEM, NorESM1-M, IPSL-CM5A-LR, GFDL-ESM2M and HadGEM2-ES.

The target global mean temperature changes were obtained by pattern-scaling the GCM projections. The pattern-scaling technique (implemented here using the ClimGen software application) (Osborn et al. 2016) assumes that there is an approximately linear relationship between the change in a climate variable in a grid cell and the change in the global-mean surface temperature, and that this relationship is invariant under the range of climate changes being considered here. This is a commonly used method and James et al. (2017) reviewed its application to global warming targets in comparison with other methods. Osborn et al. (2018) show that this method emulates the underlying GCM projections well with errors that are small relative to the climate change signal, and Tebaldi and Arblaster (2014) show that errors are small relative to the spread in results between different GCMs.

To derive future regional climate change scenarios at 0.5° latitude by 0.5° longitude resolution, scaled climate change patterns were diagnosed from 5 alternative regional climate change patterns (corresponding to 5 alternative Coupled Model Intercomparison Project (CMIP5) general circulation model (GCM) patterns). This was necessary because GCMs have not been run for the precise warming levels used in this study. To obtain the monthly time-series we combined the observed mean climate over a 30 year reference period (1961–1990), with the pattern-scaled changes (anomalies) in mean climate between 1961–1990 and a future 30-year period (2086–2115), so that the observational record provides realistic climate variability (Osborn et al. 2016). Observed climate was taken from the CRU TS3.00 dataset on a 0.5° latitude by 0.5° longitude grid (Harris et al. 2014). For future precipitation, the observed monthly anomalies were first transformed so that their probability distribution is consistent with the changes in monthly precipitation variability projected by each GCM (see Osborn et al. 2016 for details). Monthly ET was calculated using the Penman–Monteith formula from ClimGen data for minimum, maximum

and mean temperature, vapour pressure, cloud cover, and the CRU CL 2.0 wind speed climatology.

To produce daily time-series, we superimposed daily anomalies from the WATCH dataset (Weedon et al. 2011) over monthly series generated by ClimGen. WATCH is a bias-corrected reanalysis dataset designed for driving impact models and it was selected because it is compatible with the ISI-MIP fast track project (Warszawski et al. 2014) which compared many impact models across multiple sectors and it is compatible with our observational dataset. The use of present-day daily anomalies from WATCH to disaggregate the future monthly time series assumes that the daily timescale variability is unchanged in the future climate. For precipitation, the monthly variability does change in our projections (see above) and this will result in some changes in daily variability too (e.g. between anomalously wet and dry months).

2.2 Model description

The HBV (Hydrologiska Byråns Vattenbalansavdelning) model (Bergström 1992; Lindström et al. 1997) was applied in this study. It is a conceptual rainfall runoff model that has been widely used for flood forecasting and climate impact assessment both in operations and research (Lidén and Harlin 2000; Olsson and Lindström 2008; van Pelt et al. 2009; Arheimer et al. 2011; Cloke et al. 2013). There are many versions of the HBV model. The one used here is based on the HBV-IWS model (He et al. 2011) and has been adapted to be spatially distributed. HBV is computational efficient and demonstrates robust performance in catchments across the world with various climatic and physiographic conditions (e.g. Deelstra et al. n.d.; Zhang and Lindström 1996; Hundecha and Bárdossy 2004; te Linde et al. 2008; Steele-Dunne et al. 2008; Breuer et al. 2009; Driessen et al. 2010; Plesca et al. 2012; Gebrehiwot et al. 2013; Beck et al. 2013, 2016; Demirel et al. 2015; Vetter et al. 2015; Jenicek et al. 2018). HBV runs at a daily time step and the required input data include daily time series of precipitation (P) and temperature (T), and potential evapotranspiration (ET). The model was calibrated against the observed discharge data obtained from the Global Runoff Data Centre (GRDC).

The HBV model is driven by the meteorological inputs described in Section 2.1 and simulates runoff depth over each grid of 0.5×0.5 degree. This is then used to drive the CaMa-Flood (Catchment-based Macro-scale Floodplain) model (Yamazaki et al. 2011) to simulate streamflow, flood inundation depth and extent. It is a global-scale hydrodynamic model of all rivers, wetlands and lakes on the Earth and provides explicit representation of flood stage (water level and flooded area) which allows flood damage assessment by overlaying it with socio-economic datasets (Yamazaki et al. 2011). It is highly computational efficient and has been used in a number of studies on quantifying impacts of global warming on streamflows and floods (Hirabayashi and Kanai 2009; Pappenberger et al. 2012; Hirabayashi et al. 2013; Koirala et al. 2014). The relationship between water storage, water level and flooded area in the model is simulated on the basis of the subgrid-scale topographic parameters based on 3-s resolution digital elevation model. Horizontal water transport is calculated using a shallow water equation with a local inertial approximation, which realises the backwater effect in flat river basins. In this study, the CaMa-Flood model routes the gridded runoff generated by the HBV model. The spatial resolution is set at 0.25×0.25 degrees. Note, CaMa-Flood does not consider the effects of anthropogenic regulation of flood water, such as by reservoir operations or other flood defences.

2.3 Impact metrics

In this study, we assessed the changes in flood frequency and flood exposure by using the model cascade (HBV and CaMa-Flood described in Section 2.2) driven by the 5 GCMs models and 6 climate scenarios (see Section 2.1). Uncertainties due to climate model projections were assessed as the variance of the change in flood return period and population exposure driven by 5 GCMs and 6 scenarios.

A change in flood frequency between a present time period 1961–1990 (hereinafter referred to as 20C) and a future time period 2086–2115 (hereinafter referred to as 21C) was obtained as a change in the return period of a river discharge having a particular magnitude. A river discharge corresponding to a 1 in 100-year flood in 20C (hereinafter referred to as Q100-20C) was selected as the hazard indicator, in line with several previous studies (Milly et al. 2002; Hirabayashi et al. 2008, 2013; Dankers and Feyen 2008). The time series of simulated annual maximum daily river discharge in 20C for each grid, GCM and scenario were fitted respectively to a Gumbel distribution function using the maximum likelihood method. The magnitude of river discharge having a 100-year return period in 20C was then calculated. Finally, the return period of the same magnitude river discharge as the Q100-20C flood discharge was computed for the time series of 21C river discharge for each grid, GCM and scenario to project changes in future flood hazard. A decreased return period would then indicate an increase in the frequency of flood hazard.

The risks associated with the projected changes in flood hazard to human society were estimated by calculating present and future populations exposed to flood hazard. In line with previous studies (Jongman et al. 2012; Hirabayashi et al. 2013; Winsemius et al. 2016; Arnell et al. 2018) we calculated for each climate scenario the sum of the population living in the modelled inundation areas in which annual maximum discharge exceeds the Q100-20C flood. Since future exposure to fluvial flooding will be driven by both socioeconomic and climate changes also used population changes according to one of the Shared Socioeconomic Pathways (SSP2, (Jones and O’Neill 2016) as given in the spatial population scenarios dataset. In a second simulation, the population was fixed to that in 2000 to isolate the effects of climate change.

Previous studies have assessed absolute values of population at risk of flood, but are not ideal for comparisons between regions or countries as the same number of people might represent a much larger proportion of one region than in another. We thus calculated the normalised population exposure, that is the proportion of population at flooding risk by dividing the countries’ total population in 2000 (assuming population remains at the levels reached in 2000) or the total population in 2100 (assuming population growth follows SSP2). To derive changes in flood risk we then determined the difference between the proportion of the total population of each country at risk for any of our scenarios in comparison with the baseline. While this normalised population exposure metric perhaps provides a better indication of the national significance of risk levels, we also calculated the change in exposure without normalisation, so that the magnitude of the risk is also clear. This also facilitates comparison with earlier studies.

It is worth noting that (1) this study estimates large-scale (at a grid resolution of 0.25×0.25 degree) river flood risk (not pluvial, flash or coastal flooding) and (2) the CaMa-Flood model does not consider the effects of flood defences. Hence, our projection provides the potential risk of flooding, irrespective of non-climatic factors such as land-use changes, river improvements or flood mitigation efforts (Hirabayashi et al. 2013). For

places that have sufficient protection against 1 in 100-year flood, this means that some of the modelled flooding areas will in reality not be flooded and can lead to overestimation of inundation areas (Jongman et al. 2012) and population exposure.

Within each country major river basins in the Global Runoff Data Centre (GRDC 2007) database were simulated. In cases where these river basins extended beyond the border of one of our study countries the change of flooding hazard was simulated for the whole basin and the findings were clipped so that only changes of flooding risk within the country were reported.

3 Results

3.1 Projected changes in annual total precipitation and flood return periods

The projected changes in 21C in annual total precipitation (mm) and flood return period (years) for the 6 scenarios were analysed. Precipitation changes are shown first in order to facilitate understanding of the subsequent projected changes in flood risk. Figure 1a shows the changes in annual total precipitation driven by the highest warming scenario (4 °C). Decreasing annual total precipitation is projected in large areas of Brazil and Egypt, and the southern part of Ghana. India shows the highest increase in annual total precipitation, especially in the Central part. Some parts of India show decreases, most evidently in the northern side of the Himalaya ranges. China and Ethiopia show a mixed pattern of changes, indicating the changes in future flood risks could show a mixed pattern.

Figure 1b shows the return periods (years) of the discharge corresponding to the Q100-20C flood driven by the highest warming scenario (4 °C). Brazil shows an increased return period (decrease of flood frequency) in its western and some areas of its central and eastern side. In Egypt, only the grids along the Nile river display a decrease in return period. In Ghana, return periods increase in the south yet decrease in the north. In China, a large decrease in return period is projected in large areas of the western, northern and eastern part of the country, while the north-west, south-east and central areas display a mixed picture of decreasing and increasing return periods. In Ethiopia, the south-east shows large decrease in return period, and the remaining area shows a mixed pattern. In India, nearly country-wide decreasing return periods are projected except for the northern part of the Himalayan ranges.

At 1.5 °C warming, the projected median proportional area of major river basins that experience a decrease in the return period of Q100 is 47% (Brazil), 66% (China), 27% (Egypt), 65% (Ethiopia), 62% (Ghana) and 92% (India) (Fig. 2). Notably, with increasing warming, this area changes little in the cases of Egypt and India, (where only small increases to 28% and 96% are expected, respectively). In Ghana, on the other hand, the area exposed to a decrease in return period grows substantially to 86% with 4 °C warming (see Table S1 for further details).

3.2 Projected changes in population at risk from fluvial flooding

Absolute changes in population exposed to fluvial flood risk (at the Q100 level) for the six countries in 2100 are presented in Table S2. The population exposure to Q100 in 20C is listed in the fourth column. With increasing global temperatures and population change following SSP2 (chP), the population at risk from fluvial flooding is projected to increase

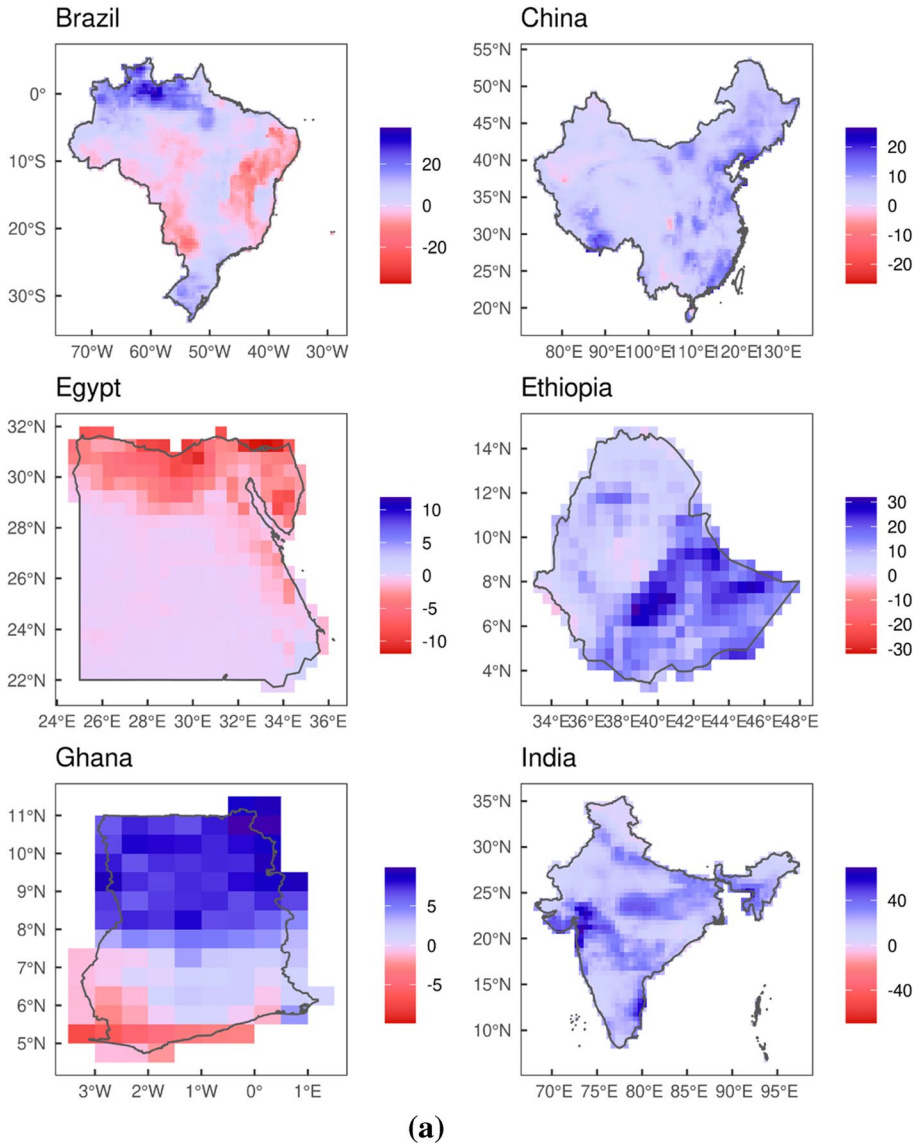
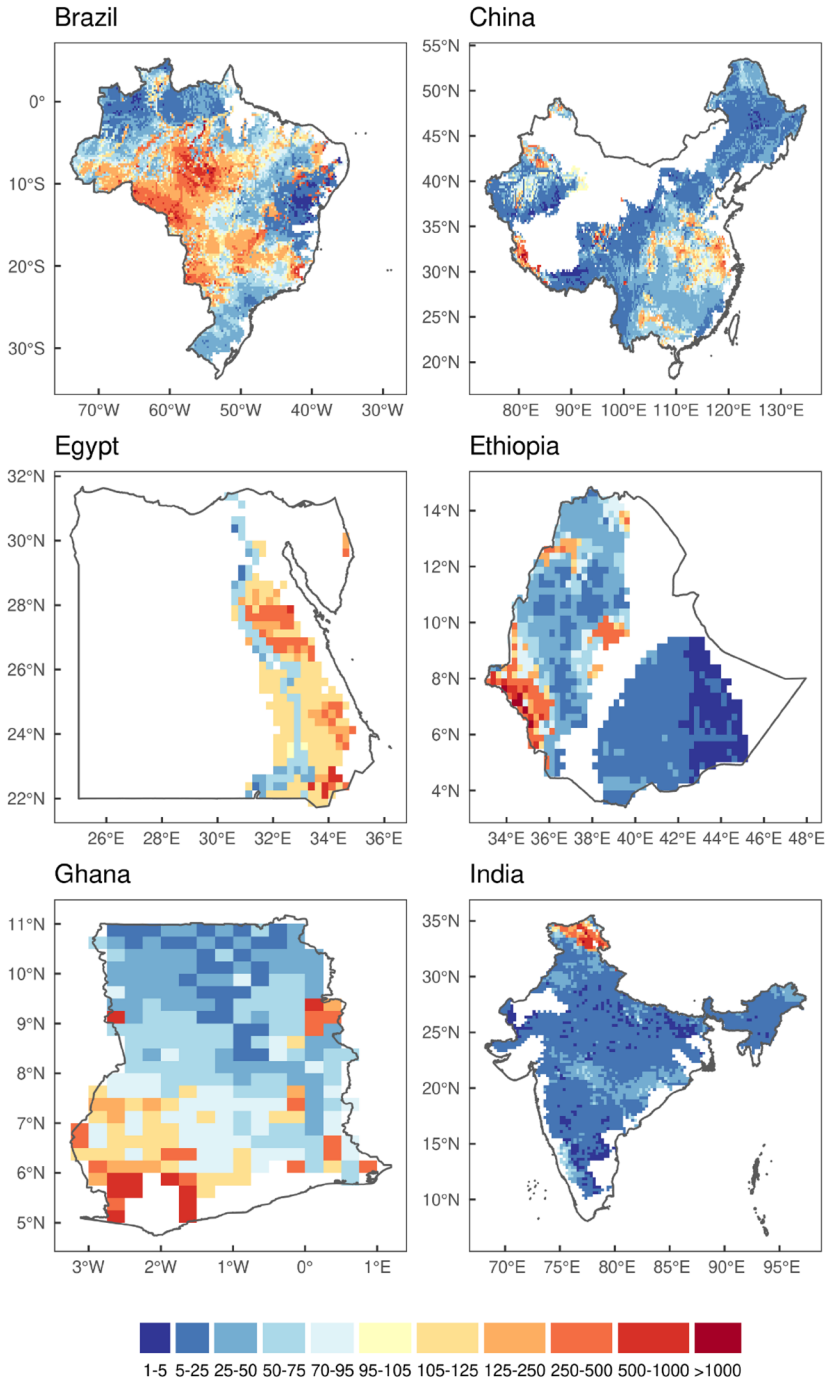


Fig. 1 (a) Projected changes of the mean annual maximum precipitation (mm) in 21C relative to 20C, and **(b)** projected return periods (years) of the discharge corresponding to the Q100-20C flood. They are both multi-model median for the 4C scenario and for each country. The white areas represent regions which were not simulated in this paper

relative to the present day (1961–1990) in all 6 countries but with stark differences between the countries. For example, with 4 °C warming, median exposure increases by 42 million people in India, whereas in Ethiopia only an increase by 85 thousand people is projected. When considering climate change alone, holding population constant (coP), risk exposure still increases with rising global temperatures but a smaller number of people are expected



(b)

Fig. 1 (continued)

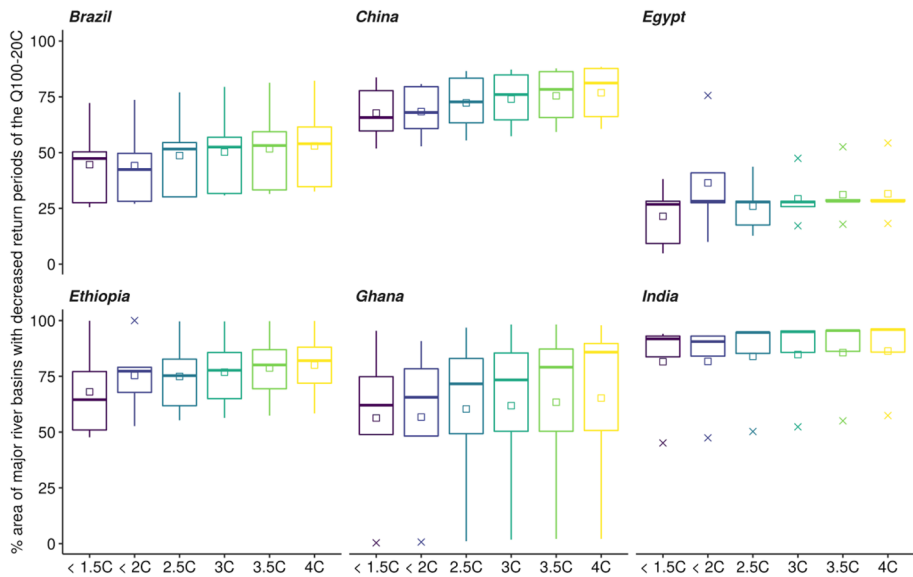


Fig. 2 Percentage (%) area of major river basins in which there is a decreased return period of the Q100-20C for the 6 countries and 6 scenarios relative to 20C. Lower and upper hinges correspond to the 25th and 75th percentile with median values given as horizontal lines. Mean values are represented as squares and points outside 1.5 times the interquartile range are highlighted as x

to be exposed in all countries but China. Looking at 4 °C warming as before, about 26 million people are now expected to be at risk in India and only about 20 thousand in Ethiopia. In China, for chP, exposure to flood risk is lower than for coP in 2100 because SSP2 projects a reduction of the population throughout China (see Figure S1 in the Supplementary Material) (Fig. 2).

We also quantified the relative changes (in percentage terms) of population at risk from fluvial flooding (Table S3). Considering both climate change and population change following SSP2, the percentage increase in potential human exposure at 4 °C relative to the observed baseline are 625% (Brazil), 111% (China), 12,083% (Egypt), 1069% (Ethiopia), 1994% (Ghana) and 4561% (India). With constant population the numbers are respectively larger in China and smaller in the remaining 5 countries (see Table S3 for more detail).

In addition to the already provided metrics, policy makers might also be interested in changes relative to the overall population of a country. We thus also normalised the changes in population exposure to the total of each country's population. The largest increases in median normalised exposure under 4 °C with changing population are 2.58% in India and the smallest are 0.04% and 0.15% in Ethiopia and Brazil, respectively (Fig. 3a). With constant population the largest increases in median normalised exposure are 1.55% in India the smallest are 0.00% and 0.14% in Ethiopia and Brazil, respectively (Fig. 3b).

Overall, projected exposure to flood risk increases steadily with global warming except in Egypt, where the increase in risk occurs mainly below 2.5 °C warming beyond which it increases but with a slower rate. However, there is substantial variability in projected change in risk between the climate models. For example, the full range of projected change in normalised risk in Egypt under 4 °C warming is –0.02 to 20.76% whereas for Ghana, it is –0.03 to 4.58%.

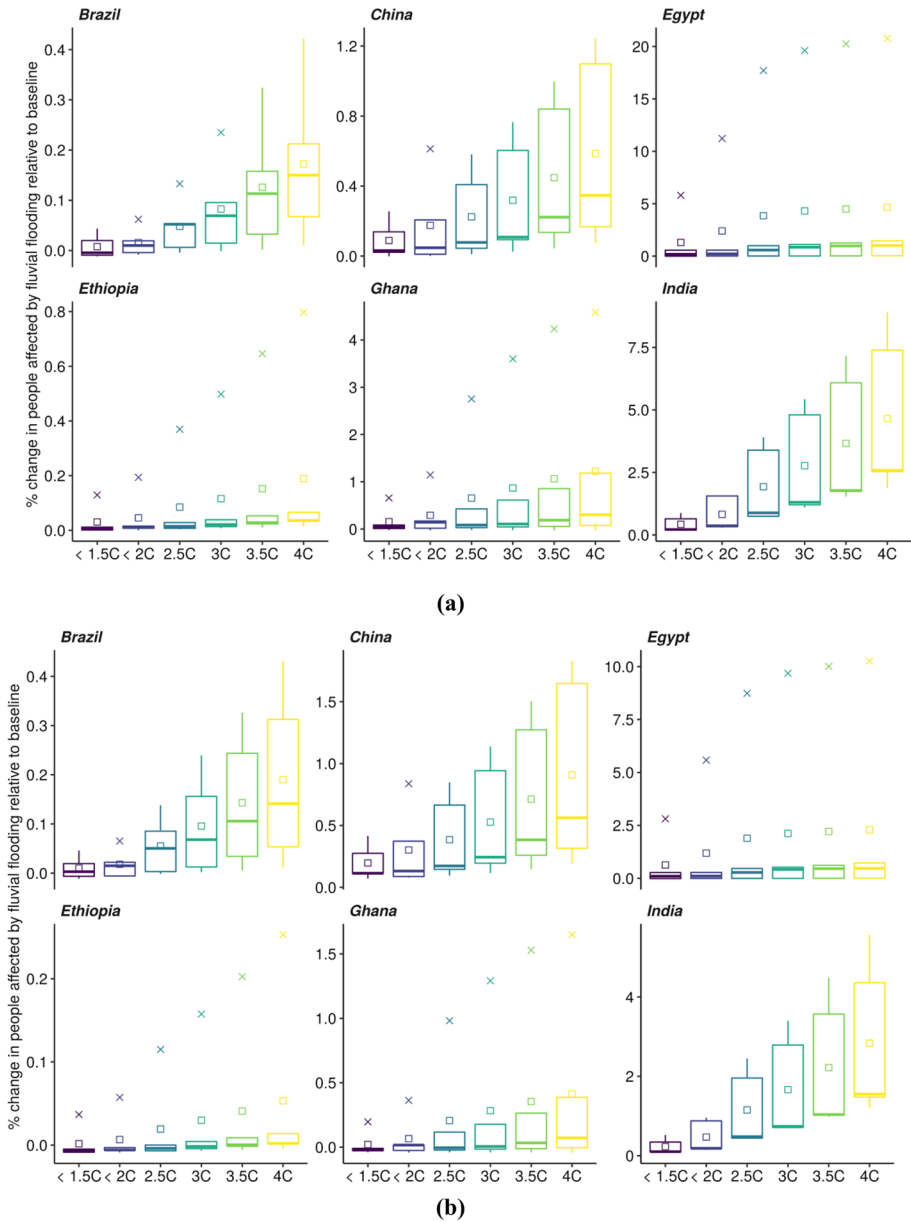


Fig. 3 Percentage (%) changes in mean annual population (normalised by the country’s total population) affected by fluvial flooding for the 6 scenarios relative to 20C **(a)** assuming population growth follows SSP2, and **(b)** assuming population remains at the levels reached in 2000

3.3 Model consistency of projected changes within each country

The model consistency of the projected changes in annual total precipitation and flood return period for the warming scenario 4C is shown in Fig. 4. If the grid value is 0 (drier

condition with strong model agreement), all 5 GCMs agree the annual total precipitation will decrease and the Q100-20C flood will be less frequent in 21C. The grid value 5 is the opposite (wetter condition with strong model agreement) when all 5 GCMs agree annual total precipitation will increase and the Q100-20C flood will be more frequent in 21C. The grid values 0 (dry) and 5 (wet) are considered consistent projection with strong (5 out of 5) agreement, 1 (dry) and 4 (wet) are moderate (4 out of 5) agreement, and 2 (dry) and 3 (wet) are low (3 out of 5) agreement.

The percentage of areas within each country with decreased return period (years) of the discharge corresponding to the Q100-20C flood shown is summarised and shown in Fig. 2. The multi-model medians of projected changes with 1.5–4 °C warming are 47–54% (Brazil), 66–81% (China), 27–28% (Egypt), 65–82% (Ethiopia), 62–86% (Ghana) and 92–96% (India). Considering only cases where there is moderate to strong model agreement, with 1.5–4 °C warming, the percentage of each country's major river basins where increasing Q100 flood frequency is projected is 83–89% (India), 55–68% (Ethiopia), 53–66% (China), 14–22% (Ghana), 9–19% (Brazil) and 3–10% (Egypt).

In Brazil, only a small portion of grids, mostly in the central-west, show the 5 GCMs agree the annual total precipitation will decrease in 21C. A large portion of Brazil show a decrease with low to moderate agreement. Small areas in the north-west and south of Brazil show increasing precipitation with low to moderate agreement. A very similar spatial pattern can be observed in the changes of flooding return period.

In China, most of the north displays high model consistency of increasing precipitation with the exception of a small area in the north-west which shows decreasing precipitation with low agreement. Transiting from north to south of China, the picture changes to a mixed pattern with some areas in the south-west and south-east showing decreasing precipitation and the remaining area show increasing precipitation with low to moderate agreement. The changes in return periods follow a very similar pattern, with the central and east part of China showing a very mixed picture of either increasing or decreasing flood frequency and with various levels of model agreement.

In Egypt, it is projected to become drier in the north with mostly strong agreement, and drier in the middle with mostly low agreement, and wetter towards the south with low to moderate agreement, but with the exception of 4 grids showing decreasing precipitation with high confidence. Although mostly decreasing precipitation is projected for the country, the return periods along the Nile river show higher occurrence of floods with low to moderate agreement (only a few grids show strong agreement).

In Ethiopia, increasing precipitation is projected with mostly strong agreement except some areas in the central, north and west. A small area in the west displays decreasing precipitation with low agreement. This spatial pattern is well reflected in the changes of flood return periods. The south-east shows increasing flood frequency with mostly strong agreement. The south-west shows decreasing flood frequency with low to moderate agreement. Towards the north-west, a more mixed pattern can be observed.

In Ghana, a clear south-north divide can be observed with decreasing precipitation in the south with low to moderate agreement. The south-west shows decreasing precipitation with strong agreement. More than half of the country is projected with increasing precipitation in the middle and north with low to moderate agreement. The return periods show mostly decreasing with low to moderate agreement with the exception of some areas in south-west and some few grids dotted around the country.

In India, increasing precipitation with moderate to strong agreement dominates the country. Very small areas in the north, south-west and central-east show decreasing precipitation with low to moderate agreement. Nearly country-wide increasing flood frequency

Fig. 4 The model consistency of the projected changes in **(a)** annual total precipitation and **(b)** flood return period. The case for the warming scenario 4C above pre-industrial level is shown. The grid values range from 0 (more model agreement on drier condition) to 5 (more model agreement on wetter condition). The grid value 0 means five models agree that **a** annual total precipitation decreases, **b** floods become less frequent; 1 means four models agree **a** decreases, **b** less frequent; 2 means three models agree **a** decreases, **b** less frequent; 3 means three models agree **a** increases, **b** more frequent; 4 means four models agree **a** increases, **b** more frequent; and 5 means five models agree **a** increases, **b** more frequent

can be observed with moderate to strong agreement, already at 1.5 °C warming, except for the northern part of the Himalayan ranges showing decreasing flood frequency with strong agreement, and low agreement of increasing flood frequency in some parts of the west. Although the area exposed to additional flood risk does not increase much beyond 1.5 °C warming, the flood hazard (and hence the population exposure to flood risk) in the country continues to increase enormously as temperatures continue to rise.

4 Discussion

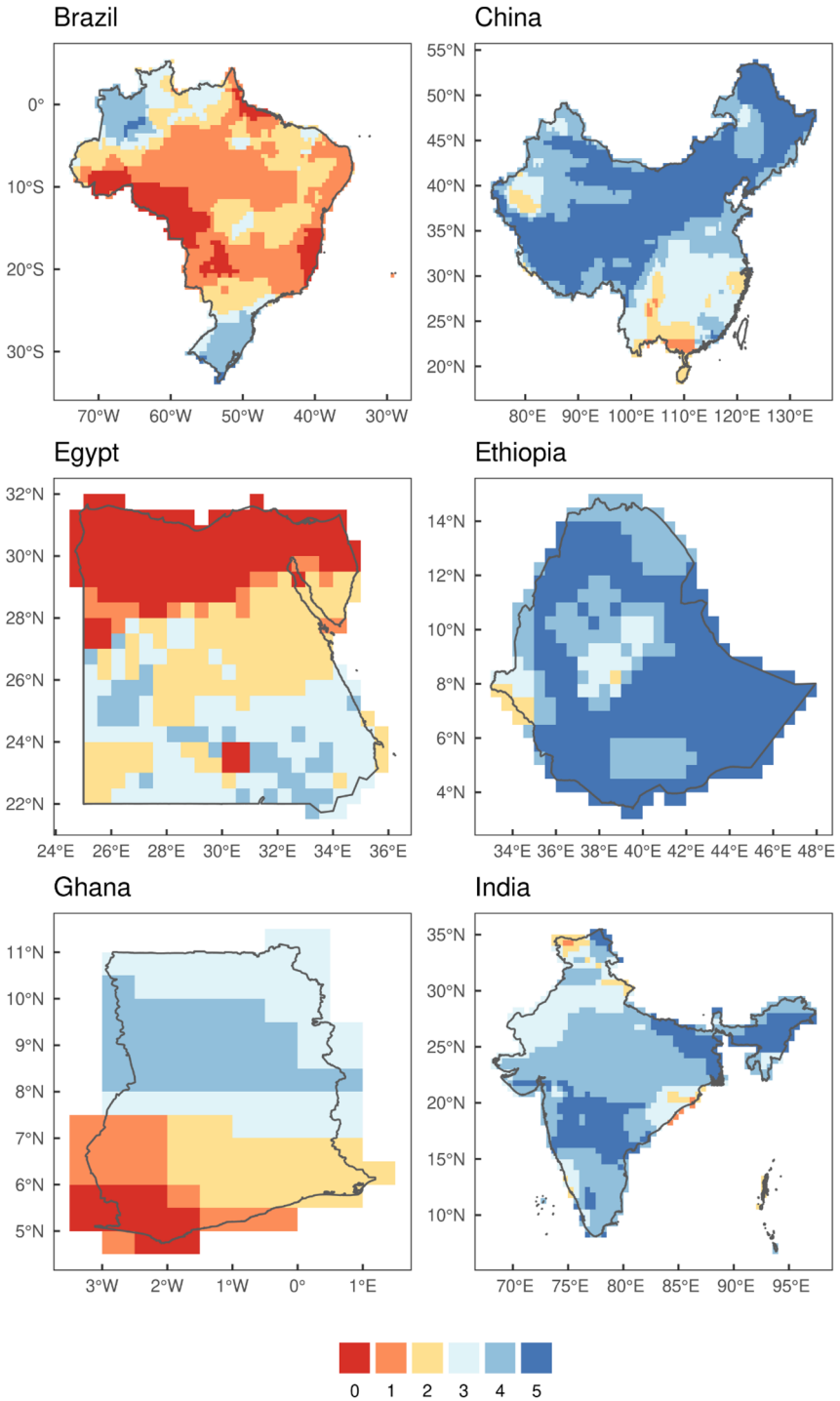
4.1 Effect of uncertainty in regional climate change projection

The uncertainty in risk projections for a specific level of warming stems from differences in climate change patterns projected by various GCMs. The results from this study were driven by 5 CMIP5 GCMs (see detail in Section 2.1). They well represent the overall spread of the 23 CMIP5 GCMs for the 6 countries (see Figure S3 in the Supplementary Material for specific details of the projected precipitation of the 23 GCMs). In general, projections of annual total precipitation in Brazil and Egypt are dominated by decreases amongst the 23 GCMs, increases in India and Ethiopia, and mixed in China and Ghana. Very large variance in the model projections for all the 6 countries can be observed.

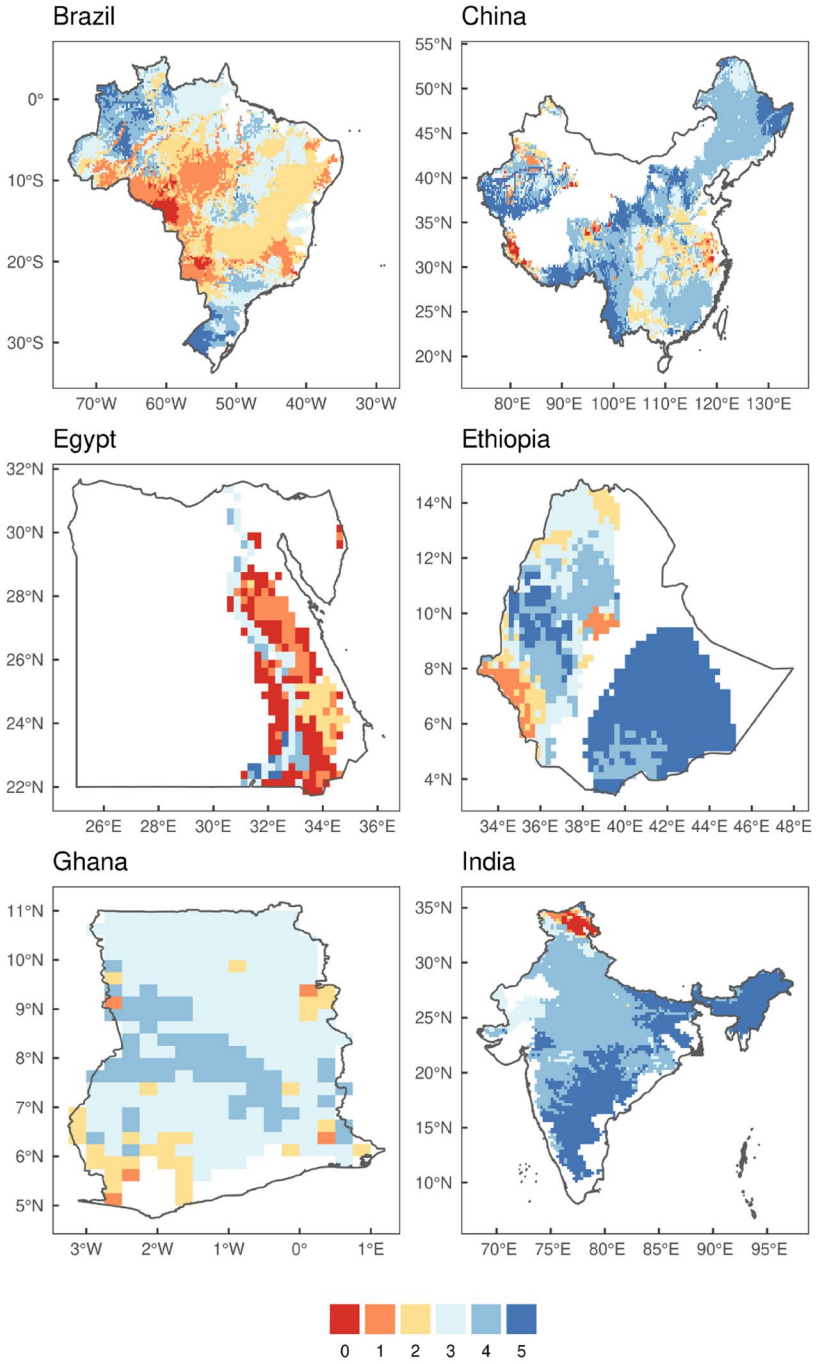
Projected changes and associated uncertainties in annual precipitation are consistent in sign with IPCC AR5 WGII Figure RC-3 (RCP8.5 late twenty-first century), also indicating that our use of a subset of five GCM patterns to diagnose future changes in precipitation samples a reasonable proportion of the overall uncertainty in modelled precipitation across the wider CMIP5 ensemble reported therein. Comparing projections across the five models, southern and eastern Brazil show divergent changes in precipitation; southern China shows divergent, or even no, change; northern Egypt shows decreasing precipitation while southern Egypt shows slight increases (although model agreement is poor); Ethiopia generally shows increasing precipitation with strong/very strong model agreement; most of Ghana shows divergent changes, while most of India shows increasing precipitation with strong or very strong model agreement.

4.2 Comparison with other studies

Most regional scale studies of the projected effects of climate change upon fluvial flood risk have focused on Europe, so few exist for the regions examined in this study. Few country level analyses of flood risk have been published that consider Ethiopia, Ghana, Brazil, or Egypt. Those available have mainly focused on China and India. Much of the previous work, globally and for specific regions, has been the results of the ISI-MIP project. Most of the existing studies project large increases in flood hazard metrics such as the return period



(a)



(b)

Fig. 4 (continued)

of Q100, the magnitude of the Q30 flood, or the population exposed to fluvial flood risk, in all of the six countries by the end of the century (Hirabayashi et al. 2013; Dankers et al. 2014; Arnell and Gosling 2016; Alfieri et al. 2017; Dottori et al. 2018). Across studies, there is a lack of agreement in the size of the increases in risk, owing mostly to the driving GCMs, the use of different hydrological models to simulate river flow (some studies do not use a hydrological or a hydrodynamic model), or the use of various metrics to indicate risk. Arnell et al. (2019a) also notes different indicators of hazard and impact are used in different global-scale studies, which makes it hard to compare results.

Many of the existing studies focus on quantification of risk in different future climate change scenarios, commonly RCP8.5 in the 2080s (e.g. Hirabayashi et al. 2013; Dankers et al. 2014; Arnell and Gosling 2016). More recent studies have set out the explicit goal to quantify the risks at specific warming levels (SWLs) (see e.g. Alfieri et al. 2017; Dottori et al. 2018; Arnell et al. 2019b, a). They variously use socio-economic assumptions ranging from no change to the selection of a particular socio-economic scenario.

Published studies of future flood risk in Ghana and Egypt mostly focus on coastal flooding rather than fluvial flooding (Apeaning Addo et al. 2011; Mahmoud and Gan 2018). Continental-level studies on projected changes in river flow across Africa report increased flood risk in Ethiopia and Ghana (Müller et al. 2014). McCartney et al. (2012) examined projected changes to the return period of floods in the Volta basin in Ghana and found some sub-basins are likely to see increases in the magnitude of higher return period floods while others are projected to experience reductions. Some studies report different signs of the change in risk using different climate and hydrological models. For example, Vetter et al. (2017) analysed large river basins across the world and found that, in China and Ethiopia, there was an inconsistency in the sign of change. Magrin et al. (2014) stated that, for much of South America, there is low confidence in projections of changes in fluvial floods due to limited evidence and complex regional variation. Studies on Brazil have so far mainly focused on pluvial floods and coastal floods (Debortoli et al. 2017). Research into projected changes in streamflow in Brazil often shows reductions in water availability and increased drought (e.g. Nóbrega et al. 2011; Montenegro and Ragab 2012). For India, Hallegate et al. (2010) and Ranger et al. (2011) projected an increase in the population affected by high return period floods. Some studies (e.g. Ying et al. 2014; Wu et al. 2017) projected an expansion of the highest flood risk areas in China, with the southeast of the country generally seeing the greatest increase in risk. Table S4 in the Supplementary Material provides a more detailed summary of the existing studies of flooding risks at a global or country level with a focus on the six countries selected in this study.

We compared our finding of changes in flood frequency with that of the study by (Hirabayashi et al. 2013). Although they used 11 CMIP5 GCMs (not including the 5 GCMs used in this study) coupled directly with CaMa-Flood and the use of RCP8.5 scenario for 21C (2071–2100) relative to 20C (1971–2000), it is considered the most comparable study given the uses of the CaMa-Flood model and the Q100 as the flood magnitude. Both studies projected increasing flood frequency along the Nile river in Egypt, nearly the whole of India, northern China and north-west of Brazil, mostly with moderate to strong model agreement. The increasing flood risk along the Nile river within Egypt is likely due to the increasing precipitation projected in the south of Egypt and its upstream countries such as Sudan and Ethiopia, even though precipitation is projected to decrease in a large part of Egypt, in particular the north with strong model agreement. There are also different findings between the two studies. Hirabayashi et al. (2013) projected increasing flood frequency in southern Ghana, most of Ethiopia and the whole of China, but we found decreasing flood frequency in southern Ghana,

some parts in the west of Ethiopia, and a very mixed pattern in north-west, south-east and central China. This could be due to the use of a completely different set of driving GCMs.

In terms of percentage change of population exposure, we compared our finding with that of the study by Alfieri et al. (2017). They used 7 CMIP5 GCMs (3 of them are included in this study) and downscaled with EC-EARTH3-HR. They used population estimates for the year 2015 from the Global Human Settlement Layer Global Population Grids (M. Pesaresi et al., 2013; S. Freire et al., 2015). With a 4C scenario, they reported 445% (Brazil), 442% (China), 170% (Egypt), 18% (Ethiopia), 54% (Ghana) and 2409% (India) increase of population exposure. We found 589%, 202%, 5662%, 254%, 624% and 2765% for the six countries, when only climate change is considered and population remains at the levels reached in 2000. For Brazil and India, the two studies have comparable numbers. Our estimates are much lower for China. It could be due to projection of decreasing flood occurrence and also disagreement in the 5 driving GCMs in some parts of the north-west, south-east and central China. Our estimates for Egypt, Ethiopia and Ghana are much higher. The population in Egypt is mostly concentrated along the Nile floodplain which coincides with the places where increased flood occurrences are projected. The model agreement is mostly low to moderate along the Nile floodplain. More driving GCMs may be required to arrive at a more robust projection. For Ethiopia and Ghana, we project much larger percentage increases of population exposure which could be a result of higher increasing flood occurrences projected in our study.

Figure S1 in the Supplementary Material shows the percentage changes of population exposure with and without population changes in 21C at the six climate scenarios. The projected population percentage changes based on SSP2 in 21C relative to the year 2000 are 12% (Brazil), -37% (China), 94% (Egypt), 203% (Ethiopia), 195% (Ghana) and 62% (India). Amongst the six countries, China is the only country with a negative population projection. It should be noted the population exposure in this study calculates the sum of the population living in the modelled inundation areas in which annual maximum discharge exceeds the Q100-20C flood. But in Alfieri et al (2017), the authors account for all floods exceeding flood protections in any given place. This means the latter accounts for multiple flooding events per year while we only account for the maximum, which translates to a much higher population exposure compared to our study. The two studies also used different population data sets for the baseline time period.

Quantification of flood risk is uncertain even in the absence of climate change. Global scale analyses variously estimate the mean annual population exposed to fluvial flooding risk in 20C to be 54 million (1976–2005) in Alfieri et al. (2017), 109 million (1995–2015) in UNISDR and CRED (2015), 5.6 million (1971–2000) in Hirabayashi et al. (2013), 805 million (1970–2005) in Jongman et al. (2012), and 81 million (1975–2001) in Jonkman (2005). It means there is a large disagreement amongst existing studies by using different time periods defined as 20C, population datasets, methods for accounting for population exposure, and methods for definitions of floods. More studies are needed to provide more estimates to build an envelope of numbers and derive a confidence interval. It also means the flood modelling community needs to agree on a common platform to work on to make results comparable.

5 Conclusion

We have applied 5 CMIP5 GCMs to drive the HBV and CaMa-Flood models at six specific warming scenarios to quantify impacts of climate and population changes on floods in the time period 21C (2086–2115) relative to the baseline time period 20C

(1961–1990). The impact measures used in this study include changes in flood return period and population exposure. The 1 in 100-year river discharge (Q100) was used as the specific flood magnitude. We projected an increase in flood frequency along the Nile river in Egypt, the whole of India, northern China and north-west of Brazil, with mostly moderate to strong model agreement. This is consistent with the results reported in IPCC AR5 WGII. We however projected decreasing flood frequency in southern Ghana, parts in the west of Ethiopia, and a very mixed pattern in north-west, south-east and central China, which is inconsistent with the results reported in IPCC AR5 WGII.

Limiting warming to 1.5 °C would greatly reduce flood risk and ultimately human exposure to floods in all of the six countries studied. At 1.5 °C warming, 47%, 66%, 27%, 65%, 62% and 92% of the major basin areas in Brazil, China, Egypt, Ethiopia, Ghana and India respectively experience a decrease in the return period of Q100-20C, rising to 54%, 81%, 28%, 82%, 86% and 96% with 4 °C warming. The decrease in return periods leads to increased human exposure to flood risks, particularly with 4 °C warming, where exposure in the major river basin areas in Brazil, China, Egypt, Ethiopia, Ghana and India increases by 589%, 202%, 5662%, 254%, 624% and 2765% relative to the 1961–1990 reference period, respectively. Limiting warming to 1.5 °C would avoid much of these increased risks, resulting in increases of 24%, 12%, 1266%, 54%, 86% and 239%.

There are a number of limitations. Firstly, there are uncertainties in our approach to climate projections. We assumed that future climate variability at the daily timescales is the same as in the present-day observations (changes in the mean climate and in the monthly timescale variability of precipitation are represented). We used simulations driven by only 5 CMIP5 model patterns. Secondly, uncertainties due to the hydrological and hydrodynamic models were not considered in this study as it is believed the uncertainties due to climate model projections dominate the total uncertainties (Kay et al. 2009; Giuntoli et al. 2015; Vetter et al. 2017; Her et al. 2019). Thirdly, the study does not consider non-climatic factors, such as flood defences and dams, and can therefore lead to over/under-estimation of inundation areas and population exposure. Using Q100 as the flood magnitude can avoid such problems in countries where flood defences are designed at protection levels lower than the 100-year return flood. Future studies can take into consideration flood protection levels to obtain more robust estimation. In addition, both current and future adaptation strategies for flooding can also affect the estimation. The FLOPROS dataset, which is an evolving global database of flood protection standards (Scussolini et al. 2016), could also add value to such impact assessment by taking flood protection standards into consideration. Fourthly, the study does not consider landcover changes. Future studies should account for land use in the model parameterisation by using possibly regionalisation techniques or other ways. Finally, the glacier runoff and snow melt in mountainous regions are not considered in this study. In future studies, a global glacier model can be added to the modelling chain to account for glacier changes and the impacts on water resources due to global warming.

We highlight the need for more detailed country or basin level studies similar to what has been undertaken in ISI-MIP but with more consistent uses of GCMs, models, time periods, population projections and more importantly impact measures. The latter will allow a better comparison within and between countries, which can provide important scientific evidence to assist policy making.

Supplementary Information The online version contains supplementary material available at <https://doi.org/10.1007/s10584-021-03289-5>.

Acknowledgements We would like to thank the members of BEIS Climate Science—International who provided feedback to the study and the manuscript. We would also like to thank the three anonymous reviewers for their careful reading of our manuscript and their insightful comments and suggestion. The observed discharge data was obtained from the Global Runoff Data Centre (GRDC).

Funding The study was funded by the UK Department for Business, Energy & Industrial Strategy (BEIS). TJO also received support from the Belmont Forum and JPI-Climate project INTEGRATE funded by the Natural Environment Research Council (grant no. NE/P006809/1). DY is funded by TOUGOU program by MEXT Japan (JPMXD0717935457).

Open Access This article is licensed under a Creative Commons Attribution 4.0 International License, which permits use, sharing, adaptation, distribution and reproduction in any medium or format, as long as you give appropriate credit to the original author(s) and the source, provide a link to the Creative Commons licence, and indicate if changes were made. The images or other third party material in this article are included in the article's Creative Commons licence, unless indicated otherwise in a credit line to the material. If material is not included in the article's Creative Commons licence and your intended use is not permitted by statutory regulation or exceeds the permitted use, you will need to obtain permission directly from the copyright holder. To view a copy of this licence, visit <http://creativecommons.org/licenses/by/4.0/>.

References

- Alfieri L, Bisselink B, Dottori F et al (2017) Global projections of river flood risk in a warmer world. *Earth's Future* 5:171–182. <https://doi.org/10.1002/2016EF000485>
- Appeaning Addo K, Larbi L, Amisigo B, Ofori-Danson PK (2011) Impacts of coastal inundation due to climate change in a cluster of urban coastal communities in Ghana, West Africa. *Remote Sens* 3:2029–2050
- Arheimer B, Lindström G, Olsson J (2011) A systematic review of sensitivities in the Swedish flood-forecasting system. *Atmospheric Res* 100:275–284. <https://doi.org/10.1016/j.atmosres.2010.09.013>
- Arnell NW, Gosling SN (2016) The impacts of climate change on river flood risk at the global scale. *Clim Change* 134:387–401. <https://doi.org/10.1007/s10584-014-1084-5>
- Arnell NW, Lowe JA, Lloyd-Hughes B, Osborn TJ (2018) The impacts avoided with a 1.5 °C climate target: a global and regional assessment. *Clim Change* 147:61–76. <https://doi.org/10.1007/s10584-017-2115-9>
- Arnell NW, Lowe JA, Bernie D et al (2019a) The global and regional impacts of climate change under representative concentration pathway forcings and shared socioeconomic pathway socioeconomic scenarios. *Environ Res Lett* 14:084046. <https://doi.org/10.1088/1748-9326/ab35a6>
- Arnell NW, Lowe JA, Challinor AJ, Osborn TJ (2019b) Global and regional impacts of climate change at different levels of global temperature increase. *Clim Change* 155:377–391. <https://doi.org/10.1007/s10584-019-02464-z>
- Beck HE, Bruijnzeel LA, van Dijk AIJM et al (2013) The impact of forest regeneration on streamflow in 12 mesoscale humid tropical catchments. *Hydrol Earth Syst Sci* 17:2613–2635. <https://doi.org/10.5194/hess-17-2613-2013>
- Beck HE, van Dijk AIJM, de Roo A et al (2016) Global-scale regionalization of hydrologic model parameters: global-scale regionalization. *Water Resour Res* 52:3599–3622. <https://doi.org/10.1002/2015WR018247>
- Bergström S (1992) The HBV model: its structure and applications. SMHI, Norrköping
- Breuer L, Huisman JA, Willems P et al (2009) Assessing the impact of land use change on hydrology by ensemble modeling (LUCHEM). I: model intercomparison with current land use. *Adv Water Resour* 32:129–146. <https://doi.org/10.1016/j.advwatres.2008.10.003>
- Cloke HL, Wetterhall F, He Y et al (2013) Modelling climate impact on floods with ensemble climate projections. *Q J R Meteorol Soc* 139:282–297. <https://doi.org/10.1002/qj.1998>
- Dankers R, Feyen L (2008) Climate change impact on flood hazard in Europe: an assessment based on high-resolution climate simulations. *J Geophys Res* 113:D19105. <https://doi.org/10.1029/2007JD009719>
- Dankers R, Arnell NW, Clark DB et al (2014) First look at changes in flood hazard in the Inter-Sectoral Impact Model Intercomparison Project ensemble. *Proc Natl Acad Sci* 111:3257–3261. <https://doi.org/10.1073/pnas.1302078110>
- Debortoli NS, Camarinha PIM, Marengo JA, Rodrigues RR (2017) An index of Brazil's vulnerability to expected increases in natural flash flooding and landslide disasters in the context of climate change. *Nat Hazards* 86:557–582. <https://doi.org/10.1007/s11069-016-2705-2>

- Deelstra J, Farkas C, Engebretsen A, et al. Can we simulate runoff from agriculture dominated watersheds? Comparison of the DrainMod, SWAT, HBV, COUP and INCA models applied for the Skuterud catchment. *Bioforsk FOKUS 5* (6), 119–128
- Demirel MC, Booiij MJ, Hoekstra AY (2015) The skill of seasonal ensemble low-flow forecasts in the Moselle River for three different hydrological models. *Hydrol Earth Syst Sci* 19:275–291. <https://doi.org/10.5194/hess-19-275-2015>
- Di Baldassarre G, Viglione A, Carr G et al (2013) Socio-hydrology: conceptualising human-flood interactions. *Hydrol Earth Syst Sci* 17:3295–3303. <https://doi.org/10.5194/hess-17-3295-2013>
- Dottori F, Szewczyk W, Ciscar J-C et al (2018) Increased human and economic losses from river flooding with anthropogenic warming. *Nat Clim Change* 8:781–786. <https://doi.org/10.1038/s41558-018-0257-z>
- Driessen TLA, Hurkmans RTWL, Terink W et al (2010) The hydrological response of the Ourthe catchment to climate change as modelled by the HBV model. *Hydrol Earth Syst Sci* 14:651–665. <https://doi.org/10.5194/hess-14-651-2010>
- Gebrehiwot SG, Seibert J, Gärdenäs AI et al (2013) Hydrological change detection using modeling: half a century of runoff from four rivers in the Blue Nile Basin: hydrological change detection using modeling. *Water Resour Res* 49:3842–3851. <https://doi.org/10.1002/wrcr.20319>
- Giuntoli I, Vidal J-P, Prudhomme C, Hannah DM (2015) Future hydrological extremes: the uncertainty from multiple global climate and global hydrological models. *Earth Syst Dyn* 6:267–285. <https://doi.org/10.5194/esd-6-267-2015>
- GRDC (2007) Major River Basins of the World. Global Runoff Data Centre, GRDC Koblenz., Germany: Federal Institute of Hydrology (BfG).
- Hallegatte S, Ranger N, Bhattacharya S, et al (2010) Flood risks, climate change impacts and adaptation benefits in mumbai: an initial assessment of socio-economic consequences of present and climate change induced flood risks and of possible adaptation options. OECD Environment Working Papers, No. 27, OECD Publishing, Paris, <https://doi.org/10.1787/5km4hv6wb434-en>.
- Harris I, Jones PD, Osborn TJ, Lister DH (2014) Updated high-resolution grids of monthly climatic observations—the CRU TS3.10 Dataset: updated high-resolution grids of monthly climatic observations. *Int J Climatol* 34:623–642. <https://doi.org/10.1002/joc.3711>
- He Y, Bárdossy A, Zehe E (2011) A catchment classification scheme using local variance reduction method. *J Hydrol* 411:140–154. <https://doi.org/10.1016/j.jhydrol.2011.09.042>
- Her Y, Yoo S-H, Cho J et al (2019) Uncertainty in hydrological analysis of climate change: multi-parameter vs. multi-GCM ensemble predictions. *Sci Rep* 9:1–22. <https://doi.org/10.1038/s41598-019-41334-7>
- Hirabayashi Y, Kanai S (2009) First estimate of the future global population at risk of flooding. *Hydrol Res Lett* 3:6–9. <https://doi.org/10.3178/hrl.3.6>
- Hirabayashi Y, Kanai S, Emori S et al (2008) Global projections of changing risks of floods and droughts in a changing climate. *Hydrol Sci J* 53:754–772. <https://doi.org/10.1623/hysj.53.4.754>
- Hirabayashi Y, Mahendran R, Koirala S et al (2013) Global flood risk under climate change. *Nat Clim Change* 3:816–821. <https://doi.org/10.1038/nclimate1911>
- Huang S, Hattermann FF, Krysanova V, Bronstert A (2013) Projections of climate change impacts on river flood conditions in Germany by combining three different RCMs with a regional eco-hydrological model. *Clim Change* 116:631–663. <https://doi.org/10.1007/s10584-012-0586-2>
- Hundecha Y, Bárdossy A (2004) Modeling of the effect of land use changes on the runoff generation of a river basin through parameter regionalization of a watershed model. *J Hydrol* 292:281–295. <https://doi.org/10.1016/j.jhydrol.2004.01.002>
- James R, Washington R, Schleussner C-F et al (2017) Characterizing half-a-degree difference: a review of methods for identifying regional climate responses to global warming targets: characterizing half-a-degree difference. *Wiley Interdiscip Rev Clim Change* 8:e457. <https://doi.org/10.1002/wcc.457>
- Jenicek M, Seibert J, Staudinger M (2018) Modeling of future changes in seasonal snowpack and impacts on summer low flows in alpine catchments. *Water Resour Res* 54:538–556. <https://doi.org/10.1002/2017WR021648>
- Jones B, O'Neill BC (2016) Spatially explicit global population scenarios consistent with the Shared Socio-economic Pathways. *Environ Res Lett* 11:084003. <https://doi.org/10.1088/1748-9326/11/8/084003>
- Jongman B, Ward PJ, Aerts JCJH (2012) Global exposure to river and coastal flooding: long term trends and changes. *Glob Environ Change* 22:823–835. <https://doi.org/10.1016/j.gloenvcha.2012.07.004>
- Jonkman SN (2005) Global perspectives on loss of human life caused by floods. *Nat Hazards* 34:151–175. <https://doi.org/10.1007/s11069-004-8891-3>
- Kay AL, Jones DA (2012) Transient changes in flood frequency and timing in Britain under potential projections of climate change. *Int J Climatol* 32:489–502. <https://doi.org/10.1002/joc.2288>

- Kay AL, Davies HN, Bell VA, Jones RG (2009) Comparison of uncertainty sources for climate change impacts: flood frequency in England. *Clim Change* 92:41–63. <https://doi.org/10.1007/s10584-008-9471-4>
- Koirala S, Hirabayashi Y, Mahendran R, Kanae S (2014) Global assessment of agreement among stream-flow projections using CMIP5 model outputs. *Environ Res Lett* 9:064017. <https://doi.org/10.1088/1748-9326/9/6/064017>
- Kundzewicz ZW, Kanae S, Seneviratne SI et al (2014) Flood risk and climate change: global and regional perspectives. *Hydrol Sci J* 59:1–28. <https://doi.org/10.1080/02626667.2013.857411>
- Lidén R, Harlin J (2000) Analysis of conceptual rainfall–runoff modelling performance in different climates. *J Hydrol* 238:231–247. [https://doi.org/10.1016/S0022-1694\(00\)00330-9](https://doi.org/10.1016/S0022-1694(00)00330-9)
- Lindström G, Johansson B, Persson M et al (1997) Development and test of the distributed HBV-96 hydrological model. *J Hydrol* 201:272–288. [https://doi.org/10.1016/s0022-1694\(97\)00041-3](https://doi.org/10.1016/s0022-1694(97)00041-3)
- Magrin GO, Marengo JA, Boulanger J-P, et al (2014) Central and South America. In: Barros VR, Field CB, Dokken DJ, et al. (eds) *Climate change 2014: impacts, adaptation, and vulnerability. Part B: regional aspects. Contribution of Working Group II to the Fifth Assessment Report of the Intergovernmental Panel of Climate Change*. Cambridge University Press, Cambridge, United Kingdom and New York, NY, USA, pp 1499–1566
- Mahmoud SH, Gan TY (2018) Urbanization and climate change implications in flood risk management: developing an efficient decision support system for flood susceptibility mapping. *Sci Total Environ* 636:152–167. <https://doi.org/10.1016/j.scitotenv.2018.04.282>
- McCartney M, Forkuor G, Sood A, et al (2012) The water resource implications of changing climate in the Volta River Basin. International Water Management Institute (IWMI), Colombo, Sri Lanka
- Milly PCD, Wetherald RT, Dunne KA, Delworth TL (2002) Increasing risk of great floods in a changing climate. *Nature* 415:514–517. <https://doi.org/10.1038/415514a>
- Montenegro S, Ragab R (2012) Impact of possible climate and land use changes in the semi arid regions: A case study from North Eastern Brazil. *J Hydrol* 434–435:55–68. <https://doi.org/10.1016/j.jhydrol.2012.02.036>
- Müller C, Waha K, Bondeau A, Heinke J (2014) Hotspots of climate change impacts in sub-Saharan Africa and implications for adaptation and development. *Glob Change Biol* 20:2505–2517. <https://doi.org/10.1111/gcb.12586>
- Nóbrega MT, Collischonn W, Tucci CEM, Paz AR (2011) Uncertainty in climate change impacts on water resources in the Rio Grande Basin, Brazil. *Hydrol Earth Syst Sci* 15:585–595. <https://doi.org/10.5194/hess-15-585-2011>
- Olsson J, Lindström G (2008) Evaluation and calibration of operational hydrological ensemble forecasts in Sweden. *J Hydrol* 350:14–24. <https://doi.org/10.1016/j.jhydrol.2007.11.010>
- Osborn TJ, Wallace CJ, Harris IC, Melvin TM (2016) Pattern scaling using ClimGen: monthly-resolution future climate scenarios including changes in the variability of precipitation. *Clim Change* 134:353–369. <https://doi.org/10.1007/s10584-015-1509-9>
- Osborn TJ, Wallace CJ, Lowe JA, Bernie D (2018) Performance of pattern-scaled climate projections under high-end warming. Part I: surface air temperature over land. *J Clim* 31:5667–5680. <https://doi.org/10.1175/JCLI-D-17-0780.1>
- Pappenberger F, Dutra E, Wetterhall F, Cloke HL (2012) Deriving global flood hazard maps of fluvial floods through a physical model cascade. *Hydrol Earth Syst Sci* 16:4143–4156. <https://doi.org/10.5194/hess-16-4143-2012>
- Pesaresi M, et al (2013) A global human settlement layer from optical HR/VHR RS data: concept and first results. *IEEE J Sel Top Appl Earth Obs Remote Sens* 6(5):2102–2131. <https://doi.org/10.1109/JSTARS.2013.2271445>
- Plesca I, Timbe E, Exbrayat J-F et al (2012) Model intercomparison to explore catchment functioning: results from a remote montane tropical rainforest. *Ecol Model* 239:3–13. <https://doi.org/10.1016/j.ecolmodel.2011.05.005>
- Ranger N, Hallegatte S, Bhattacharya S et al (2011) An assessment of the potential impact of climate change on flood risk in Mumbai. *Clim Change* 104:139–167. <https://doi.org/10.1007/s10584-010-9979-2>
- Scussolini P, Aerts JCJH, Jongman B, Bouwer LM, Winsemius HC, de Moel H, Ward PJ (2016) FLOPROS: an evolving global database of flood protection standards. *Nat Hazards Earth Syst Sci* 16:1049–1061. <https://doi.org/10.5194/nhess-16-1049-2016>
- Steele-Dunne S, Lynch P, McGrath R et al (2008) The impacts of climate change on hydrology in Ireland. *J Hydrol* 356:28–45. <https://doi.org/10.1016/j.jhydrol.2008.03.025>
- te Linde AH, Aerts JCJH, Hurkmans RTWL, Eberle M (2008) Comparing model performance of two rainfall-runoff models in the Rhine basin using different atmospheric forcing data sets. *Hydrol Earth Syst Sci* 12:943–957. <https://doi.org/10.5194/hess-12-943-2008>

- Tebaldi C, Arblaster JM (2014) Pattern scaling: its strengths and limitations, and an update on the latest model simulations. *Clim Change* 122:459–471. <https://doi.org/10.1007/s10584-013-1032-9>
- UNISDR, CRED (2015) The human cost of weather-related disasters 1995–2015. UN Off Disaster Risk Reduct UNISDR Cent Res Epidemiol Disasters CRED Geneva Switz 30
- van Pelt SC, Kabat P, ter Maat HW, Weerts AH (2009) Discharge simulations performed with a hydrological model using bias corrected regional climate model input. *Hydrol Earth Syst Sci* 13:2387–2397. <https://doi.org/10.5194/hess-13-2387-2009>
- Veijalainen N, Lotsari E, Alho P et al (2010) National scale assessment of climate change impacts on flooding in Finland. *J Hydrol* 391:333–350. <https://doi.org/10.1016/j.jhydrol.2010.07.035>
- Vetter T, Huang S, Aich V et al (2015) Multi-model climate impact assessment and intercomparison for three large-scale river basins on three continents. *Earth Syst Dyn* 6:17–43. <https://doi.org/10.5194/esd-6-17-2015>
- Vetter T, Reinhardt J, Flörke M et al (2017) Evaluation of sources of uncertainty in projected hydrological changes under climate change in 12 large-scale river basins. *Clim Change* 141:419–433. <https://doi.org/10.1007/s10584-016-1794-y>
- Warszawski L, Frieler K, Huber V et al (2014) The Inter-Sectoral Impact Model Intercomparison Project (ISI-MIP): Project framework. *Proc Natl Acad Sci* 111:3228–3232. <https://doi.org/10.1073/pnas.1312330110>
- Weedon GP, Gomes S, Viterbo P et al (2011) Creation of the WATCH forcing data and its use to assess global and regional reference crop evaporation over land during the twentieth century. *J Hydrometeorol* 12:823–848. <https://doi.org/10.1175/2011JHM1369.1>
- Winsemius HC, Aerts JCJH, van Beek LPH et al (2016) Global drivers of future river flood risk. *Nat Clim Change* 6:381–385. <https://doi.org/10.1038/nclimate2893>
- Wu Y, Zhong P, Xu B et al (2017) Changing of flood risk due to climate and development in Huaihe River basin, China. *Stoch Environ Res Risk Assess* 31:935–948. <https://doi.org/10.1007/s00477-016-1262-2>
- Yamazaki D, Kanae S, Kim H, Oki T (2011) A physically based description of floodplain inundation dynamics in a global river routing model: floodplain inundation dynamics. *Water Resour Res* 47:9726. <https://doi.org/10.1029/2010WR009726>
- Ying X, Bing Z, Bo-Tao Z et al (2014) Projected flood risks in China based on CMIP5. *Adv Clim Change Res* 5:57–65. <https://doi.org/10.3724/SP.J.1248.2014.057>
- Zhang X, Lindström G (1996) A comparative study of a Swedish and a Chinese hydrological model. *J Am Water Resour Assoc* 32:985–994. <https://doi.org/10.1111/j.1752-1688.1996.tb04067.x>

Publisher's Note Springer Nature remains neutral with regard to jurisdictional claims in published maps and institutional affiliations.